Molecular Crystals and Liquid Crystals

Publication details, including instructions for authors and subscription information:
http://www.tandfonline.com/loi/gmcl20

Small-Angle X-Ray Analysis of Smectic a Cholesteric Liquid Crystal Phase Transition in Rigid-Rod Helical Polysilane

Kento Okoshi [a b c], Anubhav Saxena [a c], Michiya Fujiki [a c], Goro Suzaki [b c], Junji Watanabe [b c] & Masatoshi Tokita [b]

[a] Graduate School of Materials Science, Nara Institute of Science and Technology, 8916-5 Takayama, Ikoma, Nara, 630-0101, Japan

[b] Department of Polymer Chemistry, Tokyo Institute of Technology, Tokyo, Ookayama, Meguro-ku, 152-8552, Japan

[c] CREST-JST (Japan Science and Technology Corporation), 4-1-8 Hon-cho, Kawaguchi, Saitama, 332-0012, Japan

Version of record first published: 18 Oct 2010

To cite this article: Kento Okoshi, Anubhav Saxena, Michiya Fujiki, Goro Suzaki, Junji Watanabe & Masatoshi Tokita (2004): Small-Angle X-Ray Analysis of Smectic a Cholesteric Liquid Crystal Phase Transition in Rigid-Rod Helical Polysilane, Molecular Crystals and Liquid Crystals, 419:1, 57-68

To link to this article: http://dx.doi.org/10.1080/15421400490478281

Mol. Cryst. Liq. Cryst., Vol. 419, pp. 57–68, 2004

ISSN: 1542-1406 print/1563-5287 online
DOI: 10.1080/15421400490478281

Taylor & Francis
Taylor & Francis Group

SMALL-ANGLE X-RAY ANALYSIS OF SMECTIC A CHOLESTERIC LIQUID CRYSTAL PHASE TRANSITION IN RIGID-ROD HELICAL POLYSILANE

*Kento Okoshi**
Graduate School of Materials Science, Nara Institute of Science and Technology, 8916-5 Takayama, Ikoma, Nara 630-0101, Japan
and
Department of Polymer Chemistry, Tokyo Institute of Technology, Ookayama, Meguro-ku, Tokyo 152-8552, Japan
and
CREST-JST (Japan Science and Technology Corporation), 4–1–8 Hon-cho, Kawaguchi, Saitama 332-0012, Japan

Anubhav Saxena and Michiya Fujiki
Graduate School of Materials Science, Nara Institute of Science and Technology, 8916-5 Takayama, Ikoma, Nara 630-0101, Japan
and
CREST-JST (Japan Science and Technology Corporation), 4–1–8 Hon-cho, Kawaguchi, Saitama 332-0012, Japan

Goro Suzaki and Junji Watanabe
Department of Polymer Chemistry, Tokyo Institute of Technology, Ookayama, Meguro-ku, Tokyo 152-8552, Japan
and
CREST-JST (Japan Science and Technology Corporation), 4–1–8 Hon-cho, Kawaguchi, Saitama 332-0012, Japan

Masatoshi Tokita
Department of Polymer Chemistry, Tokyo Institute of Technology, Ookayama, Meguro-ku, Tokyo 152-8852, Japan

The author thank Prof. Shuichi Nomura at the Tokyo Institute of Technology and Prof. Satoshi Tanimoto at the university of Shiga Prefecture for their generous support on the SR-SAXS experiments, and CREST-JST for funding the project.

*Author for correspondence. Present address, Yashima Super-structured Heliex Project, ERATO, Japan Science and Technology Corporation (JST), 101 Creation Core Nagoya, 2266-22 Anagahora, Shimoshidami, Moriyama-ku, Nagoya 463-0003, Japan. E-mail: kokoshi@yp-jst.jp

The smectic A Cholesteric liquid crystal phase transition of rigid-rod helical polysilane was studied by means of synchrotron radiation small-angle X-ray scattering (SR-SAXS). The information on the smectic trans-layer electron density distribution was clarified by fitting the model of electron density distribution to the diffraction data. Each of the layers was approximated by the box-like function to introduce the molecular form factor of the polymer. The distribution of the molecular center of gravity within the layers due to the thermal motion was taken into consideration by convolution with the Gaussian function. The elucidated smectic layer structure was not like the conventional structure with their ends packed into the interlayer space. The layers with bumpy surfaces interdigitate in a key-and-keyhole manner to pack the molecules with different lengths into layers due to their finite molecular weight distribution.

Keywords: box model; cholesteric; liquid crystal; phase transition; polysilane; smectic A

INTRODUCTION

The smectic A nematic liquid crystal phase transition is the most intensely studied liquid crystalline phase transition experimentally, and especially theoretically, from the viewpoint of the rodlike molecular model.

In the 1970s, McMillan and Kobayashi individually extended the Maier-Saupe mean field theory to evaluate the free energy of the smectic A phase, assuming a sinusoidal density distribution of the molecular center of gravity along the layer normal to describe the smectic A nematic phase transition behavior [1–4]. Indeed, subsequent experimental studies reproduced the theoretical prediction, revealing that the rodlike molecular model can reasonably depict the phase transition behavior of conventional liquid crystals with mesogenic cores and aliphatic tails [4–6].

The smectic ordering in rigid-rod particle systems, which can be assumed to be actual rods without tails, has been reported with some viruses and polypeptides [7–10]. These can be ideal systems to evaluate the efficiency of the model; however, its phase transition behavior has not been reported so far.

Very recently, we reported a columnar smectic A cholesteric phase sequence with a second-order–like smectic A cholesteric transition found in the thermotropic system of rigid-rod helical polysilane with very narrow molecular weight distribution [11–12]. Due to the severe steric requirement of neighboring chiral side chains, the polymer main chain adopts a rigid helical conformation so that it acts as a rod [13]. A typical polysilane that shows the phase sequence is poly[*n*-decyl-(*S*)-2-methylbutylsilane] (PD2MBS), with the following formula:

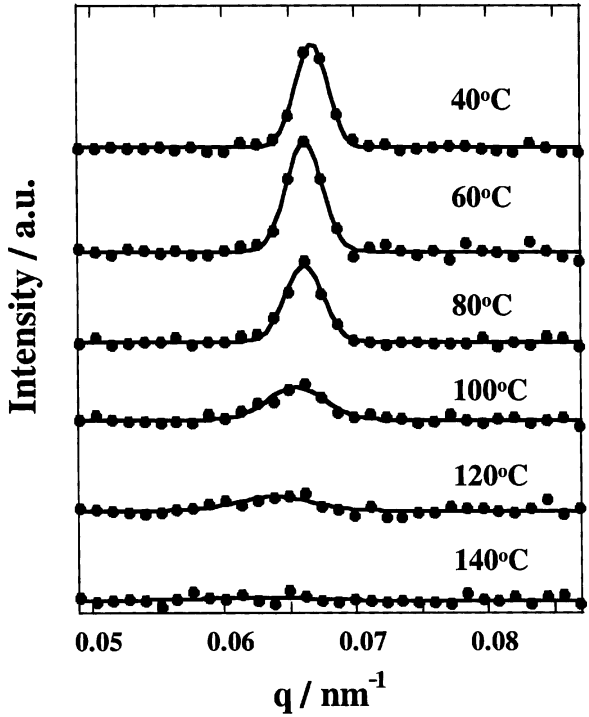

FIGURE 1 Corrected SR-SAXS profiles of PD2MBS with Mw = 18,800 and Mw/Mn = 1.11 taken at designated temperature over the smectic A cholesteric phase transition temperature. The samples were annealed at designated temperature for 30 min before measurement. Solid lines are Gaussian function fitted to the data for the purpose of guide for eyes.

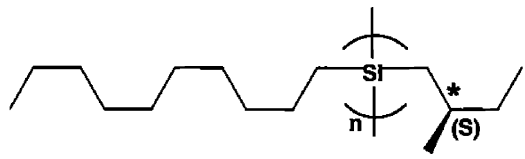

In this article, we discuss the temperature variation of the smectic A trans-layer structure of PD2MBS with narrow but finite molecular weight distribution at around its smectic A cholesteric phase transition temperature by means of synchrotron radiation small-angle X-ray scattering (SR-SAXS), which affords decisive information on the one-dimensional density wave of the smectic A layer structure, leading to elucidation of the phase

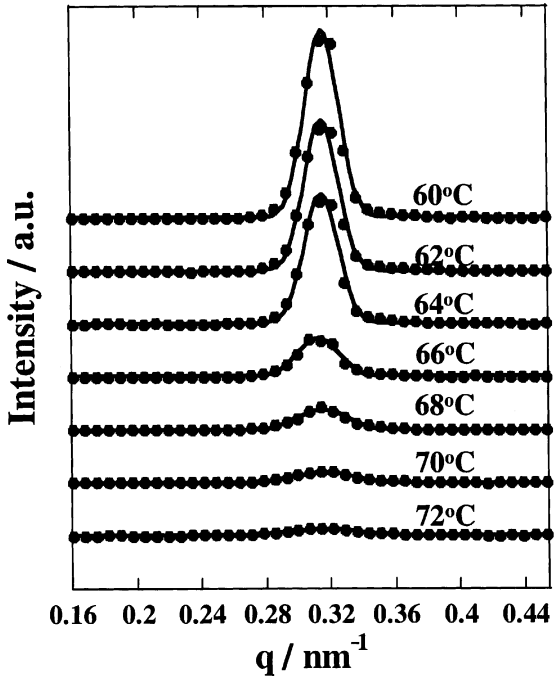

FIGURE 2 Corrected WAXD profiles of 8OCB taken at designated temperature over the smectic A nematic phase transition temperature. The samples for these measurements were kept in a glass capillary tube and annealed at designated temperature for 30 min in a Mettler FP82 hot stage before measurement. Solid lines are Gaussian function fitted to the data for the purpose of guide for eyes.

transition mechanisms peculiar to the rigid-rod particle system with finite polydispersity.

EXPERIMENTAL

Sample Preparation

The detailed synthetic procedure of PD2MBS has previously been reported [11,14]. The polymers obtained were carefully fractionated from a toluene solution with 2-propanol, ethanol, and methanol as precipitants to isolate the samples with narrow molecular weight distributions. The resulting samples were characterized by GPC (JASCO CO1560) with Shodex K-200K, at 40°C in chloroform (Nacalai Tesque, Kyoto, Japan) as an eluent, based on a calibration by polystyrene standards.

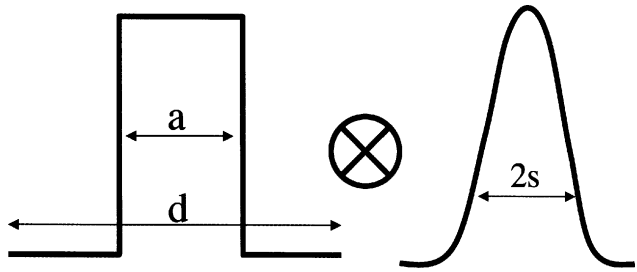

FIGURE 3 Schematic depiction of boxlike electron-density distribution model to represent the molecular form factor of PD2MBS, which is convoluted with Gaussian function to describe the distribution of the molecular center of gravity within the layers due to the thermal motion. s is the standard deviation of Gaussian function, and a and d are width of the box and layer spacing, respectively.

For a controlled experiment a typical low molecular weight liquid crystal, (n-octyloxy)cyanobiphenyl (8OCB), which has the formula

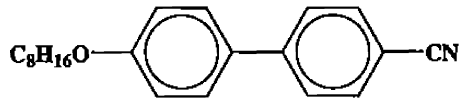

with a phase sequence of K–327.68 K–Sm A–340.37 K–N–353.39 K–Iso [15], was properly synthesized and then recrystallized three times in ethanol before use.

Measurements

The SR-SAXS experiment was carried out at the Institute of Materials Structure Science, Tsukuba, Japan (Photon Factory), with small-angel X-ray equipment installed on a beam line, BL10C, under the approval of the Photon Factory Program Advisory Committee (No. 2001G277). Details of the optics and instrumentation are described elsewhere [16]. The sample was annealed at designated temperatures for 30 min in a copper heat-block with the optical window fixed on the beam line, in which the temperature was regulated within $\pm 1^{\circ}$C, to erase the previous thermal history before measurement.

The SR-SAXS intensity was collected with point-focusing optics as an accumulation of the scattered intensity during 600 s with a one-dimensional position-sensitive proportional counter (PSPC) having an effective length of 200 mm. The scattering profiles measured by SR-SAXS were normalized for a minor decrease in the ring current during the measurement, which

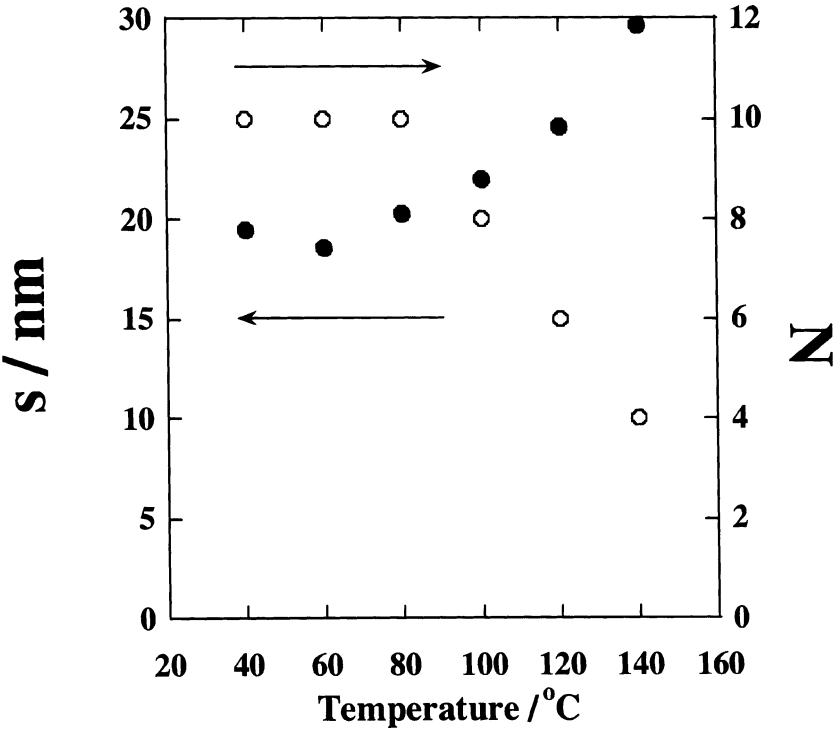

FIGURE 4 Temperature dependency of s and N evaluated with the corrected SR-SAXS diffraction profiles of PD2MBS with Mw = 18800, Mw/Mn = 1.11 over the smectic A cholesteric phase transition temperature. Filled circles and Open circles denotes s and N, respectively.

was continuously monitored by an ionization chamber placed just before the sample, and then were corrected with the calibration using the 6th reflection of collagen standard samples.

The SAXS profiles measured by SR-SAXS were then corrected for background scattering and the Lorentz factor. They were obtained as a function of q defined by

$$q = \frac{2 \sin \theta}{\lambda}, \tag{1}$$

where 2θ is the scattering angle and λ is the X-ray wavelength used, 0.1488 nm. Since the optics is of the point-focusing type, the intensity data were used without slit correction for further data treatment. We also disregarded the smearing effect by the finite cross section of the primary

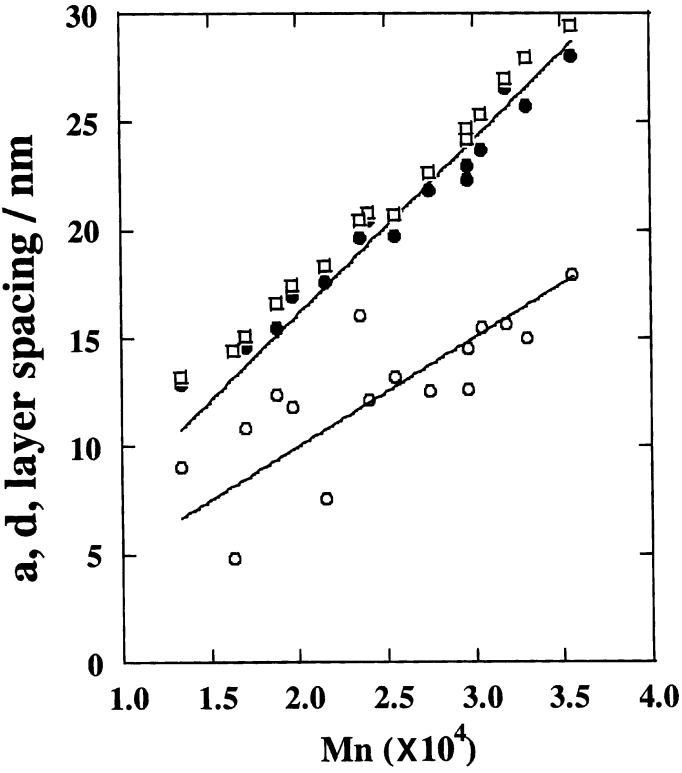

FIGURE 5 Obtained values of a, width of the box, d, layer spacing by the parameter fitting to the corrected SR-SAXS diffraction profiles of PD2MBS samples with different molecular weights and layer spacing calculated from diffraction peak position plotted against molecular weight. Open circles, filled circles, and open squares denote a, d, and layer spacing, respectively. Solid lines are linear regression function fitted to the data.

beam and sample thickness, which is convoluted with the profiles, and also the absorption factor because the reflection angle was sufficiently low.

A wide-angle X-ray diffraction (WAXD) measurement was also performed using a Rigaku-Denki X-ray generator with Ni-filtered CuK α radiation and a flat imaging plate for the low molecular weight liquid crystal, 8OCB, as a control sample, which was contained in a 1 mm Linderman glass tube. The intensity was corrected for background scattering, absorption of the sample, the geometrical effect of Laue camera, polarization, and the Lorentz factors.

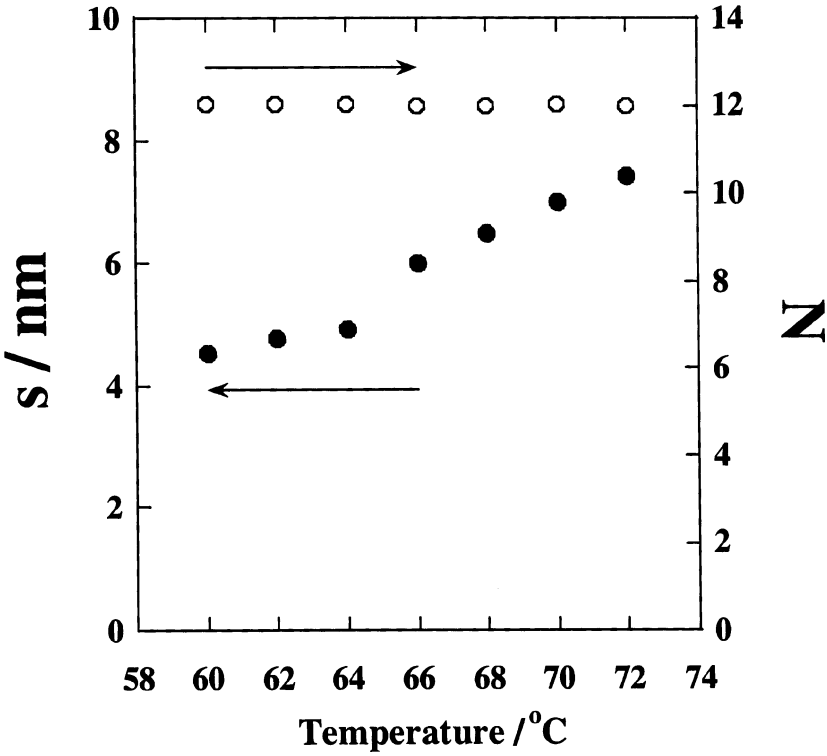

FIGURE 6 Temperature dependency of s and N evaluated with the corrected WAXD diffraction profiles of 8OCB over the smectic A nematic phase transition temperature. Filled circles and Open circles denotes s and N, respectively.

RESULTS AND DISCUSSION

Figure 1 shows the corrected SR-SAXS profiles of PD2MBS (Mw = 18800, Mw/Mn = 1.11), which display the columnar smectic A cholesteric phase sequence. The profiles were obtained at designated temperatures around the smectic A cholesteric phase transition that cannot be detected by thermal analysis. The solid lines are the Gaussian function fitted on the data for easy identification. With temperature elevation, the smectic layer reflection became diffuse, while the peak maximum of the profile shifted toward the small-angle region over the smectic A cholesteric phase transition temperature.

For comparison, corrected smectic layer reflections in WAXD profiles of 8OCB in that around the smectic A nematic phase transition are shown in Figure 2. This can be a control experiment because no substantial

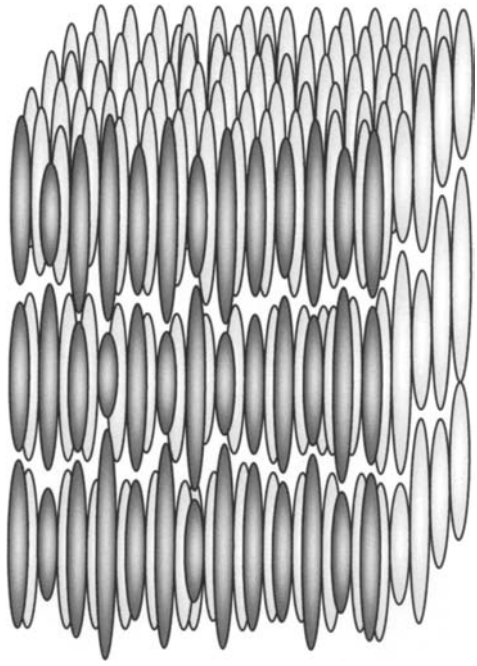

FIGURE 7 Schematic depiction of the smectic A layer structure of PD2MBS with finite molecular weight distribution.

difference has been reported between the cholesteric phase and nematic phase except chirality. There is a striking difference between PD2MBS and 80CB in that the smectic layer reflection of only 8OCB became weak without broadening (which is not the case with PD2MBS), while the reflection peak position remained unchanged on heating.

The information about the trans-layer structure can be extracted by fitting the electron density distribution model to the diffraction data. We constructed the following model of the one-dimensional electron-density distribution to be fitted to the diffraction data.

The reflection intensity $I_{real}(q)$ can be described by the Fourier-transformed electron-density distribution function, $\mathfrak{I}[\rho(r)]$, as follows:

$$I_{real}(q) = C|\mathfrak{I}[\rho(r)]|^2, \tag{2}$$

where C is a constant.

In the model, each of the layers was approximated by the boxlike electron-density distribution to introduce the molecular form factor of PD2MBS convoluted with the Gaussian function to describe the smearing

of the distribution of the molecular center of gravity within the layers due to the thermal motion, as depicted in Figure 3 [17–19].

Here, the value of s is the standard deviation of the Gaussian function: a and d are the width of the box and layer spacing, respectively; and N denotes the number of boxes and stands for the correlation length of the layers. The obtained Fourier-transformed electron-density distribution function can be seen below:

$$|\Im[\rho(r)]| = \frac{1}{\sqrt{2\pi}} \exp\left(-\frac{1}{2}s^2q^2\right) \cdot \frac{\sin(\pi aq)}{\pi q} \cdot \frac{\sin(\pi qNd)}{\sin(\pi qd)}. \tag{3}$$

To define a, the width of a box for PD2MBS, and d, its layer spacing, we carried out parameter fittings of this model, using Equations (2) and (3), to the corrected SR-SAXS profiles of PD2MBS samples with different molecular weights taken in the smectic-phase temperature region. These were carried out with s and N left open because these parameters cannot be constant for different samples due to the molecular weight dependency of the transition temperature of the polymer. The resulting a and d were plotted against the molecular weights in Figure 4, in which both of them show linearity, and d almost corresponds to the layer spacing calculated from the diffraction peak position plotted along with it. We adopted the value of $\mathrm{a/d} = 0.62$, calculated from the linear regression function in Figure 5 for further calculations of PD2MBS.

We performed a parameter fitting with the model mentioned above on the corrected SR-SAXS profiles of PD2MBS ($\mathrm{Mw} = 18800, \mathrm{Mw/Mn} = 1.11$) with an elevated temperature at around the smectic A cholesteric phase transition temperature. Figure 4 shows the temperature dependence of the obtained values of s and N. It shows that N abruptly decreases while s gradually increases with temperature elevation.

Assuming that the liquid crystal domain is sufficiently large, smectic layers gradually lose their correlation to the smectic A cholesteric phase transition, which we thought could be the origin of layer destruction. The loss of the correlation explains the peak shift toward the small-angle region, which was predicted by Hosemann's theory [20].

The parameter fitting with the same model to 8OCB was carried out with the value of $\mathrm{a/d} = 0.66$, calculated by fitting the data at 60°C, which is a well-ordered smectic A phase because the exact conformation of 8OCB in the liquid crystal state cannot be clarified. Figure 6 shows the temperature dependence of the obtained values of s and N for 8OCB.

The obtained results showed that the smectic layer order parameter of 8OCB decreased at around the smectic A nematic phase transition temperature, which was defined as the first kind of distortion in Hosemann's theory [21], while the correlation length kept constant. Evidently, it is

attributed to the thermal motion of the molecules along the layer normal, resulting in the blurring of the layer interface. However, the correlation length of PD2MBS was dramatically shortened, which was defined as the second kind of distortion in Hosemann's theory [21], while the smectic layer order parameter slightly decreases at around the transition temperature. Unquestionably, these results cannot be explained by the thermal motion of the molecules along the layer normal alone.

The decrease of the correlation length of PD2MBS is ascribed to the molecular weight distribution because a rodlike system with length distribution cannot substantially have a long-range correlation. In order to interpret the change in correlation length with the system of finite molecular weight distribution, it is an indispensable idea that the molecules are packed with their ends interdigitated at the layer interface to compensate for their molecular length distribution. In this case, the correlation length decreases with increasing temperature, probably due to random thermal molecular displacement within the layer.

In other words, molecules are packed with their center of gravity on a plane to minimize their potential energy, while their bumpy layers are interdigitated in a key-and-keyhole manner to maximize the packing entropy in the low-temperature region, as schematically depicted in Figure 7. However, with temperature increase, random molecular displacement destroys the key-and-keyhole stack and reduces the correlation length.

CONCLUSION

We elucidated the unexpected molecular packing structure of the smectic A phase of PD2MBS with a molecular weight distribution. The PD2MBS system did not form the conventional structure with their ends packed in the interlayer space to gain packing entropy as predicted by Onsager's theory.

The molecules kept their center on a plane to minimize potential energy, which is consistent with the Maier-Saupe mean field theory, while the bumpy layers stacked in a key-and-keyhole manner to gain packing entropy. The phase transition to the cholesteric phase was mainly attributed to the destruction of the stack due to the random displacement of the molecules of thermal motion.

This structure may be a plausible explanation of how rodlike molecules with a wider molecular weight distribution take the smectic A phase, and afford an explanation of the specific change in the SR-SAX diffraction profile at the phase transition.

REFERENCES

[1] Kobayashi, K. J. (1970). *Phys. Soc. Jpn.*, *29*, 101.
[2] McMillan, W. L. (1971). *Phys. Rev.*, *A4*, 1238.
[3] Kobayashi, K. (1971). *Mol. Cryst. Liq. Cryst.*, *13*, 137.
[4] McMillan, W. L. (1972). *Phys. Rev.*, *A6*, 936.
[5] Doane, J. W., Parker, R. S., Cvikl, B., Johnson, D. L., & Fishel, D. L. (1972). *Phys. Lett.*, *28*, 1694.
[6] Cabane, B. & Clark, W. G. (1973). *Sol. State Commun.*, *13*, 129.
[7] Wen, X., Meyer, R. B., & Casper, D. L. D. (1989). *Phys. Rev. Lett.*, *63*, 2760.
[8] Dogic, Z. & Fraden, S. (1997). *Phys. Rev. Lett.*, *78*, 2417.
[9] Yu, S. M., Conticello, V. P., Zhang, G., Kayser, C., Fournier, M. J., Mason, T. L., & Tirrell, D. A. (1997). *Nature*, *389*, 167.
[10] Okoshi, K., Sano, N., Suzaki, G., Tokita, M., Magoshi, J., & Watanabe, J. (2002). *Jpn. J. Appl. Phys.*, *41*, L720.
[11] Okoshi, K., Kamee, H., Suzaki, G., Tokita, M., Fujiki, M., & Watanabe, J. (2002). *Macromolecules*, *35*, 4556.
[12] Okoshi, K., Saxena, A., Naito, M., Suzaki, G., Tokita, M., Watanabe, J., & Fujiki, M. (2004). *Liq. Cryst., 31*, 279.
[13] Terao, K., Terao, Y., Teramoto, A., Nakamura, N., Terakawa, I., Sato, T., & Fujiki, M. (2001). *Macromolecules*, *34*, 2682.
[14] Fujiki, M. J. (1996). *Am. Chem. Soc.*, *118*, 7424.
[15] Sied, M. B., Lopez, D. O., Tamarit, J. Ll., & Barrio, M. (2002). *Liq. Cryst.*, *29*, 57.
[16] Ueki, T., Hiragi, Y., Kataoka, M., Inoko, Y., Amemiya, Y., Izumi, Y., Tagawa, H., & Muroga, Y. (1985). *Biophys. Chem.*, *23*, 115.
[17] Tweet, D. J., Holyst, R., Swanson, B. D., Stragier, H., & Sorensen, L. B. (1990). *Phys. Rev. Lett.*, *22*, 2157.
[18] Mol, E. A. L., Shindler, J. D., Shalaginov, A. N., & de Jeu, W. H. (1996). *Phys. Rev. E*, *54*, 536.
[19] Fera, A., Opitz, R., de Jeu, W. H., Ostrovskii, B. I., Schlauf, D., & Bahr, Ch. (2001). *Phys. Rev. E*, *64*(2–1), 021702/1.
[20] Lindenmeyer, P. H. & Hosemann, R. J. (1963). *Appl. Phys.*, *34*, 42.
[21] Bonart, R., Hosemann, R., & McCullough, R. L. (1963). *Polymer*, *4*, 199.